ELSEVIER

Carbohydrate Polymers 48 (2002) 143–152

Carbohydrate Polymers

www.elsevier.com/locate/carbpol

Interfacial tension of aqueous mixtures of Na-caseinate and Na-alginate by drop deformation in shear flow

S. Guido*, M. Simeone, A. Alfani

Dipartimento di Ingegneria Chimica, Laboratori Giovanni Astarita, Università degli Studi di Napoli Federico II, P.le V. Tecchio, 80-80125 Napoli, Italy

Received 24 November 2000; revised 16 February 2001; accepted 21 March 2001

Abstract

In this work, the interfacial tension of biphasic aqueous mixtures of Na-caseinate and Na-alginate was measured by a methodology based on drop deformation in shear flow. The two phases coexisting at equilibrium in the mixtures were separated by ultracentrifugation. A drop of one phase was injected into the other phase and sheared in a sliding plate apparatus equipped with video-enhanced microscopy. A detailed quantitative characterization of drop shape in several flow conditions, including steady state shear and transient flows, was performed by image analysis techniques. All the results are well described by classical theories of drop deformation in shear flow (which were originally developed for immiscible fluids), the only fitting parameter being the interfacial tension. The methodology used in this work allowed the measurement of very low values of interfacial tension, of the order of 10^{-5} N m^{-1}, and can be applied in general to aqueous mixtures of proteins and polysaccharides.

Keywords: Interfacial tension; Biopolymers; Drop; Shear flow; Small deformation theory

1. Introduction

Aqueous mixtures of biopolymers, such as proteins and polysaccharides, are widely used in the food industry, e.g. in the production of low- or zero-fat foods (Antonov, Grinberg, Zhuravskaya & Tolstoguzov, 1980; Blonk, Van Eendenburg, Koning, Weisenborn, & Winkel, 1995). The phase diagram of such systems is characterized by a wide miscibility gap. In this gap, the mixtures are biphasic, with each phase highly enriched with one of the two biopolymers (Antonov et al., 1980). The presence of a biphasic morphology (which can be manipulated during processing) is essential for the mixture to be able to mimic the properties of fat in food products. A key parameter governing the morphology of such mixtures and, in particular, their dependence on the flow conditions (such as those experienced during processing) is the interfacial tension between the two phases.

Even though the phase behavior of a number of protein/poysaccharide pairs in water has already been investigated (Antonov et al., 1980; Blonk et al., 1995), data on interfacial tension for only few systems are available in the literature. Examples are polyethylene glycol/dextran/water (Bamberger, Geoffrey, Seaman, Sharp & Brooks, 1984; Forciniti, Hall & Kula, 1990; Ryden & Albertsson, 1971; Wu, Zhu & Mei, 1996) and gellan/k-carrageenan/water (Wolf, Scirocco, Frith & Norton, 2000). Such scarcity of data can partly be attributed to the experimental difficulties involved in the measurement of the interfacial tension of aqueous biopolymer mixtures. In the first place, the separation of the phases coexisting at equilibrium is required. Given the close density and the rather high viscosity of the two phases, in many cases the separation process can be accomplished only by extensive ultracentrifugation of the mixture (Antonov et al., 1980; Blonk et al., 1995). Furthermore, the composition of the two phases has to be determined by analytical methods to locate the mixture on the phase diagram, since interfacial tension is expected to vary from one tie-line to the other. In particular, the interfacial tension is expected to decrease, tending to zero, as the critical point is approached. Interfacial tension is also expected to depend on molecular weight. As far as instrumentation is concerned, special experimental techniques, which allow the very low values of interfacial tension exhibited by aqueous mixtures of biopolymers to be measured in a reliable way are required.

In this work, a methodology to measure the interfacial tension of aqueous biopolymer mixtures based on drop deformation in shear flow is presented. The measuring principle is the interplay between shear-induced viscous stresses, acting to deform drop shape, and the restoring effect

* Corresponding author. Tel.: +39-081-7682271; fax: +39-081-2391800.

E-mail address: steguido@unina.it (S. Guido).

0144-8617/02/$ - see front matter
PII: S0144-8617(01)00220-X

of interfacial tension. The Na-caseinate/Na-alginate/water system was selected to illustrate the proposed techniques. Both biopolymers are widely used in the food industry and have been thoroughly investigated in the literature. A drop of one of the two coexisting phases was injected in the other phase in a parallel plate apparatus. Experimental data on drop shape, under both steady state and transient flow, were compared to classical theories of drop deformation available in the literature, the interfacial tension being the only fitting parameter. In fact, one of the main objectives of this work was to assess if classical theories, originally developed for immiscible fluids, could also be applied to biphasic mixtures. Qualitative evidence showing that some of the basic mechanisms governing the morphology of biopolymer mixtures are the same as predicted by classical emulsion theory has been provided by Foster, Underdown, Brown, Ferdinando and Norton (1997), but the polymeric nature of the system may introduce extra complications which are not accounted for in the simple emulsion approach (Qiu, Zhang & Yang, 1998). Therefore, a detailed quantitative investigation appears in order.

In the following, the Section 2 is devoted to describe the preparation of aqueous mixtures of Na-alginate and Na-caseinate, the experimental apparatus and the data analysis procedures. In Section 3, the results will be presented and discussed, and the values of interfacial tension obtained by steady state and transient data from different experiments will be compared.

2. Experimental

2.1. Materials

Na-alginate, extracted from brown seaweeds (*Macrocystis pirifera*), was purchased as powder from Sigma. Several grades, labeled according to the viscosity of a 2% (w/w) Na-alginate solution in water at 25°C, were available from the manufacturer. The Na-alginate sample used in this work was a medium viscosity grade. The molecular weight of the samples was estimated by measuring their intrinsic viscosity, according to Haug and Smidsrød (1962), and was equal to 390,000. The water content of the Na-alginate powder was determined by drying under vacuum at 70°C for 2–3 days and was about 12% (w/w). This value was used to calculate the actual concentration of Na-alginate in solution. An elemental analysis of the Na-alginate sample used in this work was kindly carried out at the Unilever research laboratories in Vlaardingen (Rob Vreeker, personal communication) and gave the following results (all the percentages are by weight): ash, 28.7% (weighed after heating at 800°C); Ca, 0.17%; Mg, 0.04%. The amount of bivalent ions was determined because they may promote the gelling of solutions of Na-alginate in water, an effect that was undesired in this work and can be excluded given the low concentrations measured. The rather high percentage of ash is partly due to the Na content (which was around 10% according to the manufacturer).

Aqueous solutions of Na-alginate were prepared by dispersing the powder in bi-distilled water ($Ca < 0.01$ mg/l) under stirring and by heating to 70°C for 30 m in order to facilitate dissolution. The solution was then cooled down to room temperature and stirred again for a few hours until complete dissolution was obtained. To prevent bacterial contamination, sodium azide was added to the solution at a concentration of 0.03% (w/w). The value of pH was adjusted to 7.0 by using NaOH 0.1 M. The adjustment was rather laborious due to the high viscosity of the Na-alginate solutions.

Na-caseinate, extracted from bovine milk, was purchased as powder from Sigma. Water content was determined by drying under vacuum at 70°C for 5 h, according to the procedure recommended by Browne (1919), and was ca. 5.5% (w/w). As before, the concentration of Na-caseinate in solution will be referred to a water-free powder. Elemental analyses of the sample investigated in this work were provided both by the manufacturer and by Unilever. The results (in weight percentages) are as follows: protein content around 90%, ash 3.8%, Na 1.2%, Ca 0.02%, Mg 0.003%.

Aqueous solutions of Na-caseinate were prepared by adding the powder in small amounts (to avoid lump formation) to bi-distilled water and stirring at room temperature. Dissolution was a slow process, especially at concentrations above 10 wt% (the highest content of Na-caseinate that could be dissolved in water was around 20 wt%). The solutions, even at low concentrations, showed a white, turbid appearance, which did not change with time. The opacity was due to the presence of minute, insoluble particles, which could be removed by centrifugation. Solutions of NaOH from 0.1 to 1 M were used to bring pH to 7.0 and the adjustment was even more time-consuming than for Na-alginate solutions, due to protein deposition on the glass electrode of the pH-meter. As for the Na-alginate solutions, sodium azide (0.03% (w/w)) was added for sample preservation.

2.2. Preparation and analysis of mixtures

Aqueous mixtures of Na-alginate and Na-caseinate were prepared by blending equal amounts of solutions of the pure components. The mixtures were stirred for several hours and then allowed to equilibrate for one day at room temperature. The value of pH was then checked again and corrected, if necessary, to 7.0. All the measurements presented in this work were carried out on mixtures of 1% (w/w) Na-alginate and 6% (w/w) Na-caseinate, which will be simply denoted as a 1–6 mixture in the following. Such mixture is well within the biphasic region according to the phase diagrams reported in the literature (Antonov et al., 1980; Blonk et al., 1995).

The 1–6 mixture looked opaque to the naked eye and a microscopic examination showed the presence of minute

drops immersed in a homogeneous continuous phase. To separate the two phases, samples of the mixture were loaded in transparent test tubes and centrifuged at 100,000 g for 15 h, keeping the temperature at 23°C. After centrifugation the samples looked clear and separated in two distinct layers, which will be referred to as the top phase and bottom phase. In order to determine the amount of each phase, the interfaces between the two layers and the air — top phase meniscus were marked on the outside of the tubes. The two phases were then carefully withdrawn by means of a syringe and stored in separate beakers for later analysis. The degree of separation achieved by centrifugation was evaluated by examining samples of the top and bottom phase under a light microscope. Each phase was free of drops, even when observed at high magnification (100 × oil immersion objective).

2.3. Rheological characterization

To determine the interfacial tension of a Na-alginate/Na-caseinate aqueous mixture by the drop deformation method, the viscosities of the coexisting phases are required. Rheological measurements on the two phases separated at 23°C from the 1–6 mixture were carried out in a controlled-stress rheometer (DSR 200, by Rheometrics) with a cone-plate configuration. The viscosity of the caseinate-rich phase at 23°C was constant with the shear rate in the complete range investigated (up to $10\ s^{-1}$), while the alginate-rich phase showed the onset of shear-thinning behavior at a shear rate around $3\ s^{-1}$. Oscillatory tests were also performed and G' and G'' were measured as a function of frequency for both phases. In all the drop deformation experiments shear rate was kept well below $1\ s^{-1}$, thus ensuring Newtonian behavior of both phases (i.e. viscosity constant with shear rate and negligible values of G').

The viscosity of the caseinate-rich phase underwent a slow, yet significant, decrease with time, reducing to about half of its initial value within a week from the date of preparation. The effect was attributed to a change of pH with time, possibly associated with the slow dissolution of protein aggregates in water. Such explanation was tested by preparing caseinate solutions in buffer tris HCl 200 mM (pH = 7.0) and it was indeed found that the viscosity remained constant with time over extended periods (more than a month). Rather than using a buffer, which might affect the value of the interfacial tension and the phase behavior, it was decided to re-measure the viscosity of the caseinate solutions each time a drop deformation experiment was performed. Such an approach is based on the assumption that interfacial tension is not significantly affected by the observed changes of viscosity with time (interfacial tension, being a measure of interactions at the interface on a molecular level, should not be sensitive to the amount of protein aggregates). Of course, the validity of this assumption will be ultimately tested by comparing values of interfacial tension measured for different values of the caseinate-rich phase viscosity. As far as the viscosity of the alginate-rich phase is concerned, some time variations were also found, but to a much lower extent that with that of the caseinate-rich phase.

2.4. Parallel-plate apparatus and drop generation

The parallel-plate apparatus used in the drop deformation experiments has been described in detail elsewhere (Guido & Simeone, 1997; Guido & Villone, 1998). Briefly, in the setup used in this work each plate is an optical glass bar of square section (100 mm × 5 mm × 5 mm), glued on a glass slide, which fits in a window cut on a rigid mount. Parallelism between the two plates is adjusted by a set of tilting, rotary and translating stages (Newport) with the aid of multiple reflections of a laser beam. Such adjustment is further refined by means of a microscope (the residual error was estimated to be about 20 μm over the whole plate length of 100 mm, i.e. less than 0.02%). One plate is displaced with respect to the other by a computer-controlled, two-axes motorized translating stage (LEP). Full travel along each of the two orthogonal axes is 100 mm (positioning accuracy: 5 μm) and the speed can be adjusted from 0.0084 to 30 mm s^{-1}.

Observations of drop deformation were performed along the vorticity direction of shear flow by using a transmitted light microscope (Axioscop FS, Zeiss), equipped with long working distance optics (20 × and 40 × objectives, Zeiss) and a zoom lens. Images were captured by a B/W CCD video camera (KP-ME1, Hitachi) and recorded on a computer-controlled VCR (AG-7355, Panasonic). The microscope was mounted on a motorized translating stage, which was used to keep the deformed drop within the field of view during shear flow. In order to minimize vibrations, the whole apparatus was placed on a vibration-isolated table (Newport) and focus was adjusted by using a motorized focus system (LEP).

A glass capillary, tapered at one end, was employed to inject a drop of one phase in the other, which had been preliminarily loaded between the parallel plates. The glass capillary was fixed to a homemade micromanipulator for precise positioning and, after drop injection, was gently extracted from the gap. To minimize edge effects from the confining surfaces of the glass slides, the gap between the plates was set at ca. 0.5 mm. Furthermore, drop diameter was at least ten times smaller than the gap (i.e. around 50 μm), in order to make wall effects negligible. Numerical simulations indeed show that wall effects become negligible when the distance between drop center and wall exceeds five times drop radius (Kennedy, Pozrikidis & Skalak, 1994; Uijttewaal & Nijhof, 1995), a condition well fulfilled in this work. Buoyancy effects were estimated by evaluating the non-dimensional quantity $\Delta\rho g R/\eta_c\dot{\gamma}$, representative of the ratio between sedimentation and shear velocity, where R is the radius of the drop at rest, η_c is the viscosity of the continuous phase and $\dot{\gamma}$ is the shear rate. According to

Phillips, Graves and Flumerfelt (1980), buoyancy effects are negligible when $\Delta\rho gR/\eta_c\dot{\gamma}$ is less than 0.3. In this work, this quantity was at most 0.01, thus ensuring that drop deformation was not affected by sedimentation.

When the drop was made of the caseinate-rich phase, it was observed that after injection in the alginate-rich phase drop size at rest slowly decreased with time. On the other hand, when a drop of the alginate-rich phase was injected in the caseinate-rich phase, a phase separation was observed inside the drop (as shown by the appearance of minute droplets within the drop). Such observations were performed at ambient temperature (about 25°C, the actual temperature being measured by a fine gauge thermocouple directly immersed in the sample). Of course, as they are likely to be associated with changes in composition, drop size variations or microscopic phase separation are undesired in this work, our aim being to measure the interfacial tension of the two phases at equilibrium corresponding to a given tie-line.

A possible explanation of these effects is that the drop was brought into contact with the other phase at a temperature slightly different from that of ultracentrifugation (23°C), i.e. under different equilibrium conditions. The temperature of the sample was then varied around 23°C (both slightly above and below), but the same effects were found. Alternative explanations are of course possible, such as non-equilibrium effects (e.g. fractionation of molecular weights) induced by the extensive ultracentrifugation required to separate the two phases. In any event, given the small size of the drop as compared to the surrounding fluid, it is clear that size variations can be caused by a rather modest driving force. So, rather than trying to find out the exact nature of the size changes, a more practical approach was adopted, i.e. an attempt was made to 'saturate' each of the two separated phases by adding a small amount of the other one. In fact, it was found that an addition of less than 1 wt% to each phase was enough to make drop size changes completely negligible on the time scale of the experiments. Such minute additions did not change the viscosity (nor, likely, the composition) of the separated phases in any appreciable way (the viscosity of the saturated phase was equal to that of the original phase within experimental error) and were therefore used in all the experiments presented in this work.

2.5. Analysis of drop shape

Quantitative parameters representative of drop shape were measured by an automated procedure based on image analysis techniques, which has been described in detail elsewhere (Guido & Villone, 1998) and will be briefly described here. Images of the deformed drop captured by the CCD video camera and recorded on videotape were digitized by an 8-bit frame grabber (Spectrum, Imagraph) installed on a Pentium II host computer. Contrast was enhanced by adjusting gain and offset of the incoming video signal prior to digitization. The images were analyzed by a Visual Basic macro, exploiting standard image analysis routines provided by a commercial software package (Image-Pro Plus 4.0, Media Cybernetics). The macro implemented an automated procedure of edge detection, based on maximization of the contrast of the drop with respect to the background while preserving a closed contour. The two axes a and b of the deformed drop (as observed in the plane of shear) and the angle θ between the major axis a and the velocity gradient direction (see the schematic drawing in Fig. 1) were calculated for an equivalent ellipse (i.e. having the same area and first and second moments of area of the actual drop). A bilinear transformation (Gonzales & Woods, 1992) was applied to correct the moments for the small distortions introduced by the video camera and the frame grabber and to convert image pixels into microns.

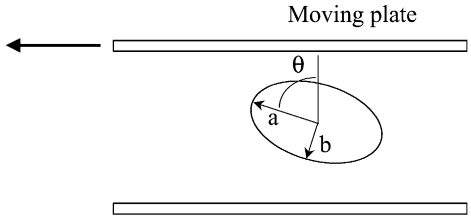

Fig. 1. A schematic drawing of a deformed drop showing the two axes a and b and the angle θ in the plane of shear.

Several small deformation theories available in the literature have been applied in this work to evaluate the interfacial tension from the experimental data of drop shape. Both steady state and transient data were used in the calculations. Steady state shape was analyzed by the well-known equation derived by Taylor (1932, 1934)

$$D = \frac{19\lambda + 16}{16\lambda + 16} Ca \tag{1}$$

relating the deformation parameter $D = (a - b)/(a + b)$ to the capillary number $Ca = \eta_c R\dot{\gamma}/\sigma$ (where σ is the interfacial tension) through a (weak) function of the viscosity ratio $\lambda = \eta_d/\eta_c$, η_d being the viscosity of the drop. Eq. (1) has been extensively tested against experimental data (de Bruijn, 1989; Guido & Villone, 1998; Rumscheidt & Mason, 1961; Taylor, 1934; Torza, Cox & Mason, 1972) and good agreement was found as long as the capillary number was low enough to fall within the small deformation limits of the theory.

An equation relating the angle θ to the capillary number under steady state conditions was first derived by Cerf (1951) and then corrected for a small error by Roscoe (1967)

$$\theta = \frac{\pi}{4} + \frac{(19\lambda + 16)(2\lambda + 3)}{80(1 + \lambda)} Ca \tag{2}$$

Eq. (2) was also later obtained by Chaffey and Brenner (1967) through an expansion of drop shape to the second order in Ca. As for Eq. (1), good agreement has been found between Eq. (2) and experimental data at low values of Ca

(Guido & Villone, 1998; Rumscheidt & Mason, 1961; Torza et al., 1972), also taking into account the difficulties associated with the measurement of θ, especially at small deformations. In the limit of vanishing Ca, θ tends to 45°, but is of course undefined for a spherical shape.

Eqs. (1) and (2) can be combined together in the following expression

$$\theta = \frac{\pi}{4} + \frac{(2\lambda + 3)}{5} D \tag{3}$$

which can be used to check the internal consistency of the measured values of D and θ. Indeed, by fitting Eq. (3) to the experimental data one can evaluate the viscosity ratio as the only fitting parameter and compare it to the value calculated from the independently measured viscosities of the two phases.

Cox (1969) developed a theoretical analysis of drop shape under shear flow and provided expressions of the deformation parameter D and the angle θ as a function of Ca and λ for both steady state conditions and start-up transients. The following are, respectively, the steady state equations for D and θ

$$D = \frac{5(19\lambda + 16)}{4(1 + \lambda)\sqrt{(19\lambda)^2 + (20/Ca)^2}} \tag{4}$$

$$\theta = \frac{\pi}{4} + \frac{1}{2} \tan^{-1}\left(\frac{19Ca\lambda}{20}\right) \tag{5}$$

and both reduce to Taylor results in the limit of vanishing Ca. The equations for the start-up transients for D and θ are as follows

$$D(t) = D_{\text{steady}}\left[1 - 2\exp\left(\frac{-20\dot{\gamma}t}{19Ca\lambda}\right)\cos(\dot{\gamma}t) + \exp\left(\frac{-40\dot{\gamma}t}{19Ca\lambda}\right)\right]^{1/2} \tag{6}$$

$$\theta(t) = \frac{\pi}{4} - \frac{1}{2}\tan^{-1}\left\{\frac{19\lambda\left[\exp\left(\frac{-20\dot{\gamma}t}{19Ca\lambda}\right)\cos(\dot{\gamma}t) - 1\right] + (20/Ca)\exp(-20\dot{\gamma}t/19Ca\lambda)\sin(\dot{\gamma}t)}{-(20/Ca)[\exp(-20\dot{\gamma}t/19Ca\lambda)\cos(\dot{\gamma}t) - 1] + 19\lambda\exp(-20\dot{\gamma}t/19Ca\lambda)\sin(\dot{\gamma}t)}\right\} \tag{7}$$

It has been shown (Torza et al., 1972) that Eq. (4) tends to underestimate the experimental values of D for increasing Ca at moderately high values of λ, while Eq. (5) fails to predict the experimental trend of θ at $\lambda \leq 1$. The most appropriate range of applicability of Cox theory is at $\lambda \gg 1$, where good agreement has been found with experimental data both for Eq. (4) (as long as Ca is low enough) and for Eq. (5) (at any value of Ca). A comparison of Cox theory with numerical simulations (Kennedy et al., 1994; Uijttewaal & Nijhof, 1995) showed the same results.

Another technique widely used to evaluate interfacial tension is based on the analysis of the retraction of a drop from a deformed configuration to the spherical shape at rest. Several methods have been proposed in the literature to analyze the shape of a retracting drop, either derived from simplified phenomenological models (Carriere & Cohen, 1991; Cohen & Carriere, 1989; Sigillo, Di Santo, Guido & Grizzuti, 1997) or based on numerical simulations (Tjahjadi, Ottino & Stone, 1994). Recently, the following simple analytical expression for the evolution of D with time during retraction has been proposed (Guido & Villone, 1999)

$$D = D_0 \exp\left(-\frac{40(\lambda + 1)}{(2\lambda + 3)(19\lambda + 16)}\frac{t\sigma}{\eta_c R}\right) \tag{8}$$

where D_0 is the value of D at the beginning of the retraction. Eq. (8) was obtained from the first order theory of Taylor according to the formulation given by Rallison (1984) and is valid only for small deformations. According to Eq. (8), data of $\ln(D/D_0)$ plotted vs time should fall on a straight line, whose slope is proportional to σ. Such a predicted trend and the values of σ so obtained are in good agreement with experimental data (Guido & Villone, 1999).

It should be noticed that Eqs. (1)–(8) are all analytical and do not contain adjustable parameters. Depending on the experimental conditions, any of these equations can be fit to the data thus allowing σ to be calculated as the only fitting parameter. The application of Eqs. (1)–(8) will be illustrated in the following section.

3. Results and discussion

All the experiments presented in this work were carried out according to the following procedure. After drop injection in the continuous phase between the parallel plates, the speed of the moving plate was set at the lowest value selected for the experiment (which was usually 0.01 mm s^{-1}). Motion was then started and the sample was sheared for a time long enough for it to reach a stationary drop shape. At this point, the flow was stopped and the drop allowed to relax back to the spherical shape. The whole sequence, including start-up and retraction upon cessation of flow, was recorded on videotape for later analysis, as described in the previous section. Speed and travel of the moving plate were then progressively increased for each of the subsequent runs, until a stationary drop shape could not be attained anymore (a condition of incipient breakup). Due to the limited travel of the moving plate, flow direction was reversed from time to time. The overall magnification was

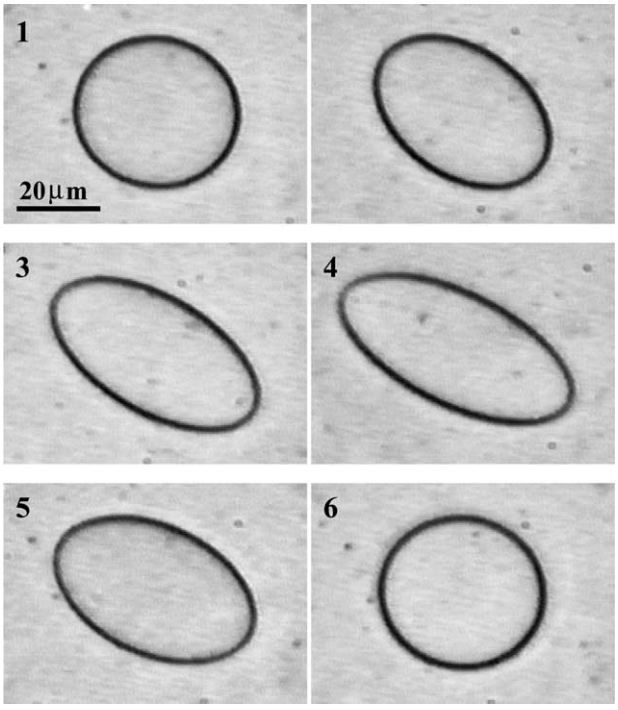

Fig. 2. A sequence of images acquired at consecutive times showing the deformation of a caseinate-rich phase drop in the alginate-rich phase (shear rate: 0.05 s^{-1}): (1) drop at rest; (2–3) start-up transient; (4) stationary shape; (5–6) retraction.

decreased in the course of the experiment by changing zoom and objectives, to make it easier to follow drop motion at higher speeds. Reproducibility was assessed by repeating the experiment ex novo, i.e. starting from the preparation of fresh solutions of Na-alginate and Na-caseinate. Furthermore, drop phase and continuous phase were also inverted.

A sequence of images from a typical experiment is presented in Fig. 2. The remainder of this section is divided in three subsections, where results from steady state, start-up and retraction will be presented.

3.1. Steady state results

In this subsection, the evaluation of the interfacial tension from steady state data of D and θ will be presented. The first step in data analysis was to check the viscosity ratio, which can be calculated by fitting Eq. (3) to a plot of θ vs D at steady state, as described in the section on drop shape analysis. In Fig. 3 the angle θ is shown as a function of D for a drop of the caseinate-rich phase in the alginate-rich phase. As described in the Section 2, a small quantity of each phase was added to the other one to avoid drop size variations with time (such additions were 0.82 wt% of the alginate-rich phase and 0.47 wt% of the caseinate-rich phase). Drop radius at rest was 25 μm and no significant change of size was observed in the course of the experiment. The viscosity ratio calculated from the viscosities of the two phases measured at the time of the experiment was 0.65 at 25°C.

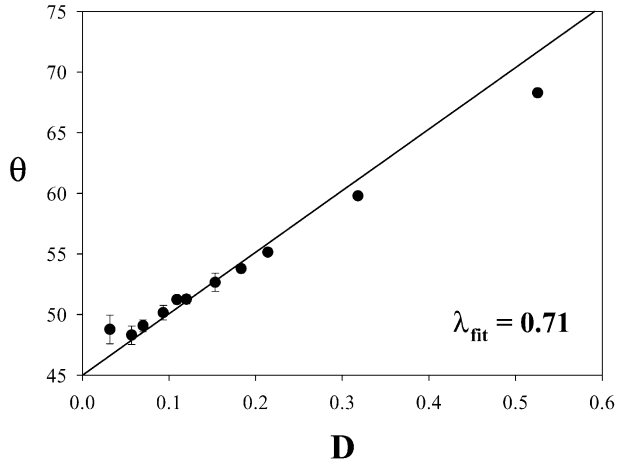

Fig. 3. Plot of the angle θ as a function of the deformation parameter D at steady state for a caseinate-rich phase drop in the alginate-rich phase. The value of λ was calculated by fitting Eq. (3) to the data (continuous line).

By fitting Eq. (3) to the data in Fig. 3 (solid line) a value of 0.71 was obtained for λ, which was the only fitting parameter (to stay within the limits of the small deformation theory, the fit was restricted to values of $D < 0.25$). This result can be considered in good agreement with the viscosity ratio independently determined from rheological data (whose experimental error, due to sample evaporation, instrumental accuracy, etc. can be estimated at around 5%), especially if the difficult handling of the materials is taken into account. The error bars in Fig. 3 correspond to the standard deviation of θ in each run, since every point was calculated as the average of several values (around 50) at steady state. The error bars are not shown for D as they are of the same size as the symbols.

In Fig. 4 D is plotted as a function of shear rate (bottom

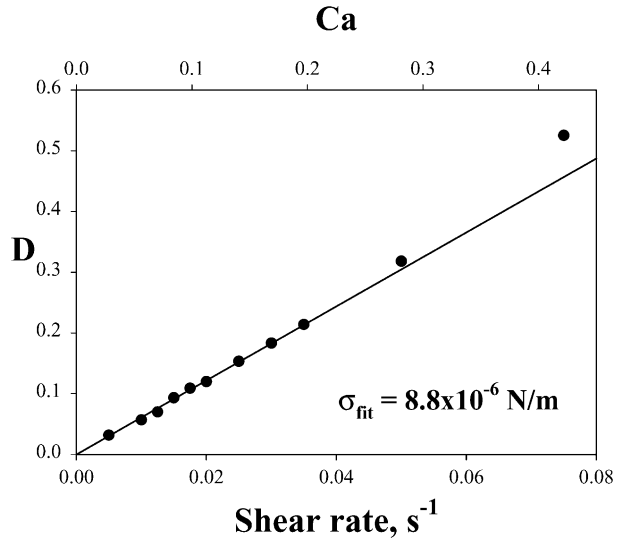

Fig. 4. The deformation parameter D as a function of the shear rate (bottom axis) for the same experiment of Fig. 3. The continuous line is the best fit of Eq. (1) to the data, with σ as the only fitting parameter. The so obtained value of σ was used to calculate the capillary number shown as the top axis.

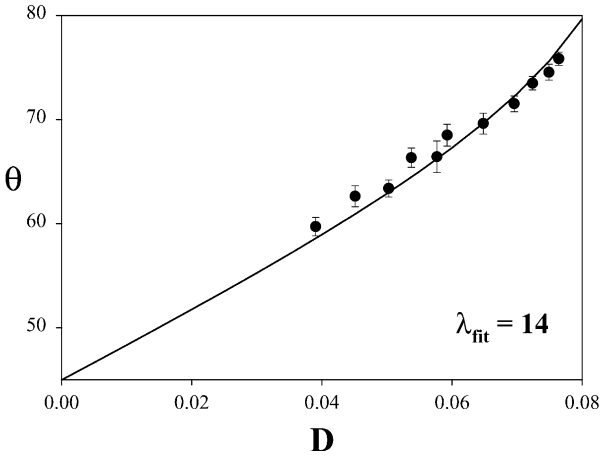

Fig. 5. Plot of the angle θ as a function of the deformation parameter D at steady state for a alginate-rich phase drop in the caseinate-rich phase. The value of λ was calculated by applying Cox theory (continuous line).

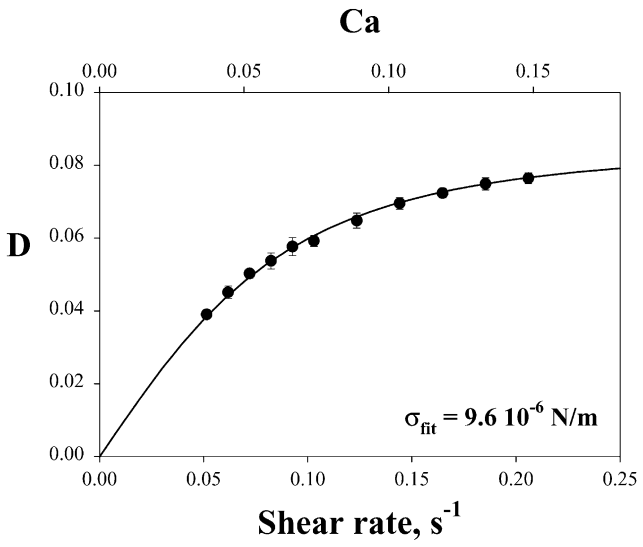

Fig. 6. The deformation parameter D as a function of the shear rate (bottom axis) for the same experiment of Fig. 5. The continuous line is the best fit of Eq. (4) to the data, with σ as the only fitting parameter. As before, the capillary number is also shown (top axis).

horizontal axis) for the same experiment as in Fig. 3. The value of interfacial tension obtained by fitting Eq. (1) to the experimental data of Fig. 4 (solid line) was 8.8×10^{-6} N m^{-1} (as in Fig. 3, only points having $D < 0.25$ were used in the fitting procedure). Having so determined σ, the capillary number can now be calculated; it is reported as the top horizontal axis of Fig. 4. As a further check, it can be noted that the data used in the evaluation of σ also correspond to $Ca < 0.25$, which is within the small deformation limit of Eq. (1) for λ around 1 (Guido & Villone, 1998).

Steady state data for a drop of the alginate-rich phase in the caseinate-rich phase are presented in Figs. 5 and 6. Here the additions made to each phase to avoid drop size variations with time were equal to 0.37 wt% of the caseinate-rich phase and 0.31 wt% of the alginate-rich phase. Drop radius at rest was 25.5 μm and no significant changes of size were found in the course of the experiment. The viscosity ratio calculated from the viscosities of the two phases measured at the time of the experiment was 12 (which is not equal to the inverse of the viscosity ratio of the experiment of Figs. 3 and 4 due to the change of the viscosity of the solutions with time). To check the value of the viscosity ratio the angle θ was plotted as a function of D, as shown in Fig. 5. It can be noticed that the data do not follow a linear trend, even though drop deformation is rather small ($D < 0.1$), a behavior characteristic of high values of λ. A linear portion of the data at low shear rates (where Eq. (6) would be applicable) cannot be easily identified in Fig. 5. Therefore, the theory of Cox, which is valid at high values of λ, was used. In particular, by combining Eqs. (4) and (5) the capillary number can be eliminated and one ends up with a relation between θ and D (not reported here for the sake of brevity), where, as for Eq. (3), the only material property is the viscosity ratio. By fitting such equation to the experimental data (solid line in Fig. 5) a value of 14 was obtained for λ, which is in reasonable agreement with the result obtained from viscosity data.

The deformation parameter D is plotted as a function of shear rate in Fig. 6. The full line was obtained by fitting Eq. (4) from the Cox model to the data, with σ as the only fitting parameter (λ was set to 14, the value obtained from Fig. 5). The result was $\sigma = 9.6 \times 10^{-6}$ N m^{-1}, which is in good agreement with the value obtained in the previous experiment with the inverted phases (the difference is about 9%). It can be noticed that the capillary number, which is shown as the top horizontal axis in Fig. 6, is lower than 0.15, a range where the Cox theory is in good agreement both with experimental data (Torza et al., 1972) and numerical simulations (Kennedy et al., 1994; Uijttewaal & Nijhof, 1995) at values of λ similar to the one of the present experiment.

3.2. Start-up transients

Shear flow start-up transients were analyzed only for the case of $\lambda \gg 1$ (i.e. when the drop was made of the alginate-rich phase) by using Cox Eqs. (6) and (7). As an example, the time evolution of the deformation parameter D during start-up at a shear rate of 0.2 s^{-1} is plotted in Fig. 7 for the same experiment as Figs. 5 and 6. It can be noticed that D exhibits an overshoot before reaching a steady state value, a trend typical of high viscosity ratios. The value of interfacial tension calculated by fitting Cox Eq. (6) to the data in Fig. 7 is 9.9×10^{-6} N m^{-1}, in close agreement with the result obtained from steady state data.

The plot of θ vs time during start-up (at the same shear rate) is presented in Fig. 8. The same qualitative features of the time evolution of D (i.e. an initial overshoot followed by a leveling off) can be observed, and the data are well represented by Cox Eq. (7), shown by the continuous curve. The resulting interfacial tension, which is 10×10^{-6} N m^{-1}, is again in good agreement with the values reported so far.

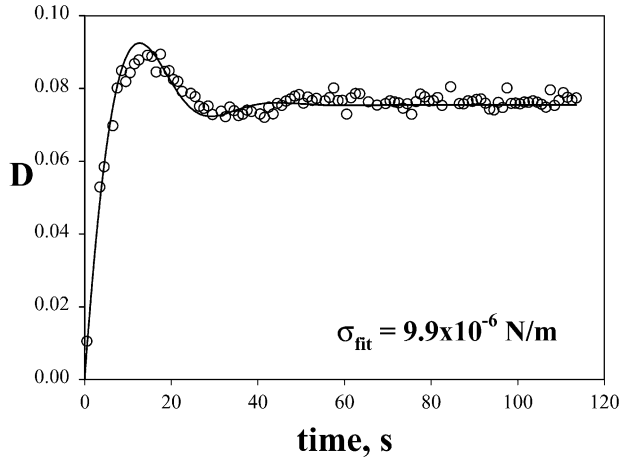

Fig. 7. Plot of D as a function of time during start-up at a shear rate of 0.2 s^{-1} (same experiment as in Figs. 5 and 6). The value of σ shown in the figure was calculated by fitting Eq. (6) to the data.

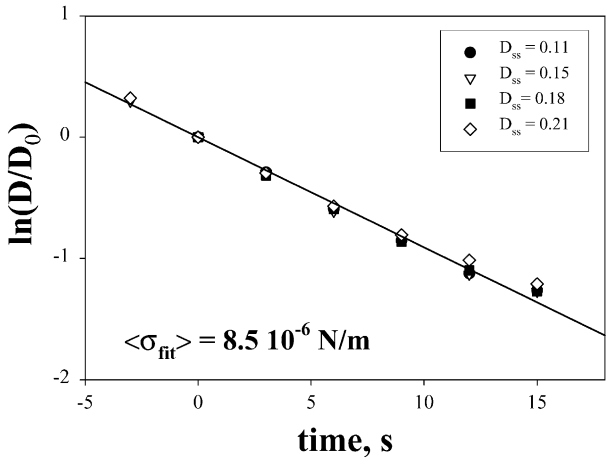

Fig. 9. Plot of $\ln(D/D_0)$ vs time during four retractions upon cessation of shear flow (same experiment as in Figs. 3 and 4). The stationary values of D are shown in the inset. In all the runs D_0 was taken equal to 0.1.

3.3. Drop retraction upon cessation of shear flow

The interfacial tension was also evaluated by fitting Eq. (8) to data of D vs time during relaxation. Drop retraction upon cessation of flow was followed for several runs from each experiment. An example is presented in Fig. 9, where $\ln(D/D_0)$ is plotted as a function of time for six retractions from the experiment of Figs. 3 and 4 (drop of caseinate-rich phase). The steady state values of D in the shear flow (prior to retraction) range from 0.1 to 0.21 and are shown in the caption. Since the validity of Eq. (8) is limited to small deformations, only the values of $D \leq 0.1$ were plotted for each retraction in Fig. 9 (i.e. D_0 was taken as equal to 0.1 for all four retractions).

It can be noticed that all the data in Fig. 9 show a linear trend, as predicted by Eq. (8). The continuous line in Fig. 9 is the plot of Eq. (8) with the average value of σ from the four retractions, which was 8.5×10^{-6} N m^{-1}, with a standard deviation of 2×10^{-7} N m^{-1}. Such a value is in good agreement with the results obtained from the steady state data presented in Figs. 3 and 4. Drop retractions in the experiments with reversed phases provided a value for σ of 8.9×10^{-6} N m^{-1}, with a standard deviation of 8×10^{-7} N m^{-1} over four retractions (the plot is not shown for the sake of brevity).

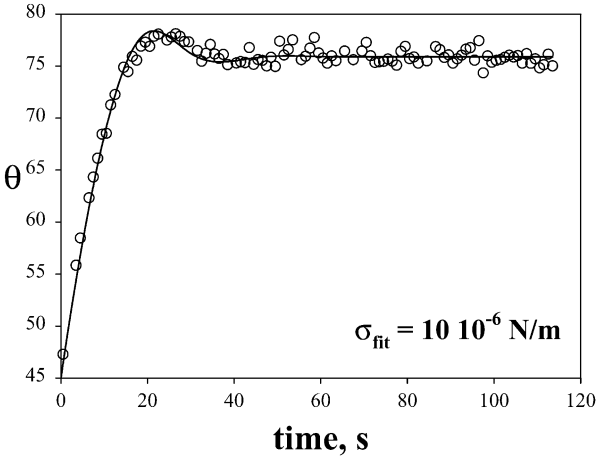

Fig. 8. Plot of θ as a function of time during start-up at a shear rate of 0.2 s^{-1} (same experiment as in Figs. 5 and 6). The value of σ shown in the figure was calculated by fitting Eq. (7) to the data.

3.4. Comparison of the different methods

In this work, apart from the two experiments which have been described so far, two more experiments (both with the drop made of the caseinate-rich phase) were carried out, in order to test the reproducibility of the experimental technique. For the sake of brevity, the data fittings of these other experiments will not be shown. The results are summarized in Table 1, where the values of interfacial tension of the 1–6 mixture calculated from the various methods illustrated in the previous subsections in all the four experiments are presented. Experiments 1 and 4 are the ones previously described in detail. The values of interfacial tension obtained from retractions and start-up transients in Table 1 correspond to the average of several runs (2–4). For a given method (e.g. steady state D), the equation used for data fitting is also reported.

The average interfacial tension obtained from the application of all the different methods is 8.9×10^{-6} N m^{-1}, with a standard deviation of 0.8×10^{-6} N m^{-1}. Such a low standard deviation shows the good reproducibility of the proposed methodology, which was tested not only by repeating the experiment, but also by exchanging continuous and dispersed phase. The value of σ found in this work cannot be compared to previous results in the literature owing to the lack of data for the system under investigation. In fact, such a lack of data was one of the motivations for performing an extensive data analysis, including the application of several methods.

Table 1

Experiment#	σ ($\times 10^6$ N m^{-1})		
	Steady state D Eq. (1)	Retraction Eq. (8)	
Drop: caseinate-rich phase			
1	8.8	8.5	
2	9.3	8.4	
3	9.4	7.4	
	Steady state D Eq. (4)	Retraction Eq. (8)	Start-up Eqs. (6) and (7)
Drop: alginate–rich phase			
4	9.6	8.9	9.9

4. Conclusions

The main result of this work is the development of an experimental methodology to measure the interfacial tension of aqueous biopolymer mixtures. The proposed approach is based on the analysis of the shape assumed by a drop of one phase of the mixture immersed in the other phase under the action of shear flow, in both steady state and transient conditions. The methodology was applied to the Na-caseinate/Na-alginate/water system, for which no data on interfacial tension are available in the literature.

An issue thoroughly addressed in this work is testing the applicability of classical theories of drop deformation, which were developed for pure immiscible fluids, to the case of biphasic biopolymer mixtures. For this purpose, theoretical expressions were fit to data of both D and θ under different flow conditions. It was found that in all experiments, as far as the condition of small deformation is satisfied, drop shape was well described by such theories, with interfacial tension as the only fitting parameter. Furthermore, the values of σ so determined were all in good agreement. In general, better results can be expected from the application of the equations involving the deformation parameter D (in particular Eq. (1), which is rather insensitive to errors in the value of λ), since this quantity can be measured with higher accuracy, even at small deformations, as compared to the angle θ. In any case, it should be pointed out that the equation to be used depends on both the value of λ and the range of the available data.

One of the main advantages of drop deformation methods is the ability to measure extremely low values of interfacial tension, which would be very difficult to evaluate from conventional techniques. As an example, the spinning drop technique, which has been used to measure σ for the polyethylene glycol/dextran/water system, requires accurate values for the density difference between the coexisting phases, a measurement increasingly difficult as the critical point is approached. A drawback of the proposed methodology is the complex handling of the materials, which includes phase separation by ultracentrifugation and proper care of problems such as the decrease with time of the caseinate-rich phase viscosity and variations of drop size in the course of the experiment. As a consequence, the experiments are rather time-consuming (each experiment may require 2–3 weeks of dedicated work). In this respect, it should be pointed out that the mixtures investigated in this work are not model fluids, but complex materials extracted from biological sources.

As mentioned in Section 1, interfacial tension is a key parameter governing flow-induced morphology of liquid–liquid systems. A possible application of the results of this work is the determination of the average size of mixtures by fitting the Palierne model (1990) to rheological data under oscillatory flow, a method which requires preliminary knowledge of the interfacial tension. Work is currently in progress in this area. Furthermore, once the interfacial tension is known, predictions on the smallest drop size that can be attained in shear or extensional flow can also be made by using correlations available in the literature (de Bruijn, 1989; Grace, 1982). The results presented in this paper are restricted to liquid–liquid mixtures. A further direction of future work is the investigation of biphasic systems where (at least) one phase is in the gel state, which is a case of special interest for food applications (Wolf et al., 2000).

Acknowledgements

Financial support by the European Union under FAIR contract no. CT97-3022 is gratefully acknowledged. The authors are indebted to Prof. F. Alfani of the University of L'Aquila for performing a HPLC analysis of the Na-caseinate sample used in this work and for many helpful suggestions. The authors wish to thank Dr R. Vreeker, Dr R. de Bruijn and Dr W.G.M. Agterof of the Unilever Research Laboratorium Vlaardingen for providing the elemental analysis data for Na-alginate and Na-caseinate and for helpful discussions. Critical reading of the manuscript by Dr Bettina Wolf of the Unilever Research Colworth is also gratefully acknowledged.

References

Antonov, Y. A., Grinberg, V. Y. A., Zhuravskaya, N. A., & Tolstoguzov, V. B. (1980). Liquid two-phase water–protein–polysaccharide systems and their processing into textured protein products. *Journal of Texture Studies*, *11*, 199–215.

Bamberger, S., Geoffrey, V., Seaman, F., Sharp, K. A., & Brooks, D. E. (1984). The effects of salts on the interfacial tension of aqueous dextran poly(ethylene glycol) phase systems. *Journal of Colloid and Interface Science*, *99*, 194–200.

Blonk, J. C. G., Van Eendenburg, J., Koning, M. M. G., Weisenborn, P. C. M., & Winkel, C. (1995). A new CSLM-based method for determination of the phase behavior of aqueous mixtures of biopolymers. *Carbohydrate Polymers*, *28*, 287–295.

Browne, F. L. (1919). The proximate analysis of commercial casein. *Journal of Industrial and Engineering Chemistry*, *11*, 1019–1024.

de Bruijn, R. A. (1989). *Deformation and breakup of drops in simple shear flows*. PhD thesis, Technische Universiteit Eindhoven.

Carriere, C. J., & Cohen, A. (1991). Evaluation of the interfacial tension between high molecular weight polycarbonate and PMMA resins with the imbedded fiber retraction technique. *Journal of Rheology*, *35*, 205–212.

Cerf, R. J. (1951). Recherches théoriques et expérimentales sur l'effet Maxwell des solutions de macromolécules déformables. *Journal de Chimie Physique*, *48*, 59–84.

Chaffey, C. E., & Brenner, H. (1967). A second-order theory for shear deformation of drops. *Journal of Colloid and Interface Science*, *24*, 258–269.

Cohen, A., & Carriere, C. J. (1989). Analysis of a retraction mechanism for imbedded polymeric fibers. *Rheologica Acta*, *28*, 223–232.

Cox, R. G. (1969). The deformation of a drop in a general time-dependent fluid flow. *Journal of Fluid Mechanics*, *37*, 601–623.

Forciniti, D., Hall, C. K., & Kula, M. R. (1990). Interfacial tension of polyethyleneglycol-dextran-water systems: influence of temperature and polymer molecular weight. *Journal of Biotechnology*, *16*, 279–296.

Foster, T. J., Underdown, J., Brown, C. R. T., Ferdinando, D. P., & Norton, I. T. (1997). Emulsion behavior of non-gelled biopolymer mixtures. In E. Dickinson & B. Bergenstahl, *Food colloids: Proteins, lipids and polysaccharides* (pp. 346–356). Cambridge: RSC.

Gonzales, R. C., & Woods, R. E. (1992). *Digital image processing*, Reading, MA: Addison-Wesley.

Grace, H. P. (1982). Dispersion phenomena in high viscosity immiscible fluid systems and applications of static mixers as dispersion devices. *Chemical Engineering Communications*, *14*, 225–277.

Guido, S., & Simeone, M. (1997). Binary collisions of drops in simple shear flow by computer-assisted video optical microscopy. *Journal of Fluid Mechanics*, *357*, 1–20.

Guido, S., & Villone, M. (1998). Three dimensional shape of a drop under simple shear flow. *Journal of Rheology*, *42*, 395–415.

Guido, S., & Villone, M. (1999). Measurement of interfacial tension by drop retraction analysis. *Journal of Colloid and Interface Science*, *209*, 247–250.

Haug, A., & Smidsrød, O. (1962). Determination of intrinsic viscosity of alginates. *Acta Chemica Scandinavica*, *16*, 1569–1578.

Kennedy, M. R., Pozrikidis, C., & Skalak, R. (1994). Motion and deformation of liquid drops, and the rheology of dilute emulsions in simple shear flow. *Computers and Fluids*, *23*, 251–278.

Palierne, J. F. (1990). Linear rheology of viscoelastic emulsions with interfacial tension. *Rheologica Acta*, *29*, 204–214.

Phillips, W. J., Graves, R. W., & Flumerfelt, R. W. (1980). Experimental studies of drop dynamics in shear fields: role of dynamic interfacial effects. *Journal of Colloid and Interface Science*, *76*, 350–370.

Qiu, F., Zhang, H., & Yang, Y. (1998). Chain stretching effect on domain growth during spinodal decomposition of binary polymer mixtures under simple shear flow. *Journal of Chemical Physics*, *108*, 9529–9536.

Rallison, J. M. (1984). The deformation of small viscous drops and bubbles in shear flows. *Annual Review of Fluid Mechanics*, *16*, 45–66.

Roscoe, R. (1967). On the rheology of a suspension of viscoelastic spheres in a viscous liquid. *Journal of Fluid Mechanics*, *28*, 273–293.

Rumscheidt, F. D., & Mason, S. G. (1961). Particle motions in sheared suspensions XII. Deformation and burst of fluid drops in shear and hyperbolic flow. *Journal of Colloid and Interface Science*, *16*, 238–261.

Ryden, J., & Albertsson, P. A. (1971). Interfacial tension of dextran-polyethylene glycol-water two-phase systems. *Journal of Colloid and Interface Science*, *37*, 219–222.

Sigillo, I., Di Santo, L., Guido, S., & Grizzuti, N. (1997). Comparative measurements of interfacial tension in a model polymer blend. *Polymer Engineering and Science*, *37*, 1540–1549.

Taylor, G. I. (1932). The viscosity of a fluid containing small drops of another fluid. *Proceedings of the Royal Society of London*, *A138*, 41–48.

Taylor, G. I. (1934). The formation of emulsions in definable fields of flow. *Proceedings of the Royal Society of London*, *A146*, 501–523.

Tjahjadi, M., Ottino, J. M., & Stone, H. A. (1994). Estimating interfacial tension via relaxation of drop shapes and filament breakup. *AIChE Journal*, *40*, 385–394.

Torza, S., Cox, R. G., & Mason, S. G. (1972). Particle motion in sheared suspensions. XXVII. Transient and steady deformation and burst of liquid drops. *Journal of Colloid and Interface Science*, *38*, 395–411.

Uijttewaal, W. S. J., & Nijhof, E. J. (1995). The motion of a droplet subjected to linear shear flow including the presence of a plane wall. *Journal of Fluid Mechanics*, *302*, 45–63.

Wolf, B., Scirocco, R., Frith, W. J., & Norton, I. T. (2000). Shear-induced anisotropic microstructure in phase-separated biopolymer mixtures. *Food Hydrocolloids*, *14*, 217–225.

Wu, Y. -T., Zhu, Z. -Q., & Mei, L. -H. (1996). Interfacial tension of poly(ethylene glycol) + salt + water systems. *Journal of Chemical Engineering Data*, *41*, 1032–1035.